Original Research Article

Development of Linagliptin Ultra Fine Solid Supersaturated Bio-SNEDDS Using Triangular Mixture Design for Enhancement of Oral Bioavailability: Impact of P-gp Inhibition

LIN in clove oil

+ cremophor CO 40

+ labrasol

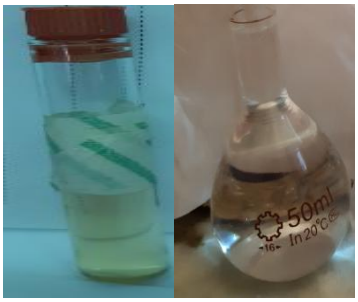

SNEDDS

Supersaturated SNEDDS

(s-SNEDDS)

Solid supersaturated SNEDDS

(Ss-SNEDDS)

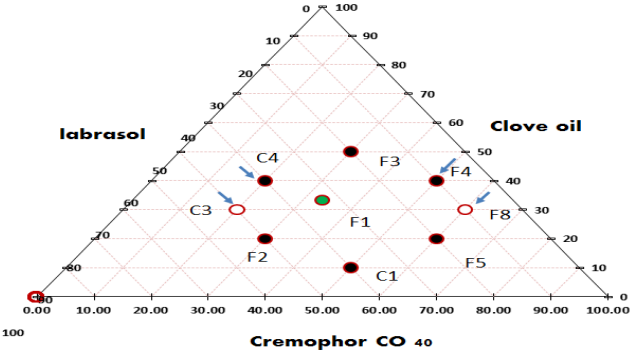

Optimization by triangular mixture design

Characterization

In vivo pharmacokinetics

In vitro release

In vitro precipitation

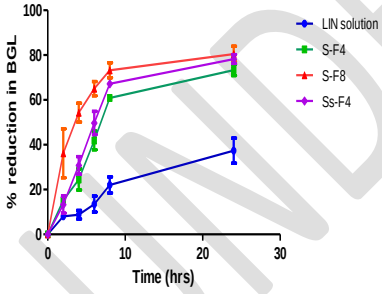

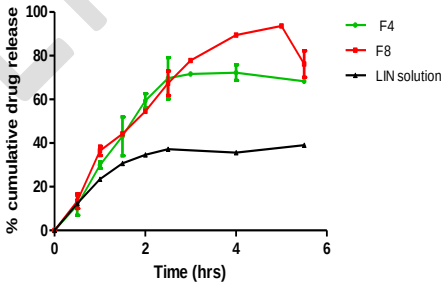

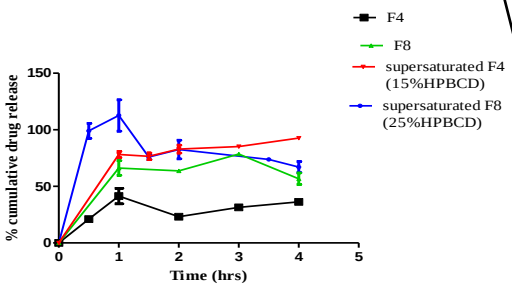

TEM

Graphical abstract

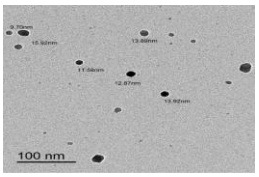

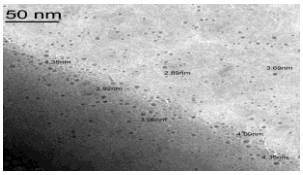

F4 **F8**

Abstract

Aims

Linagliptin (LIN) is a newly developed dipeptidyl peptidase 4 (DPP-4) inhibitor oral antidiabetic drug. LIN is considered a P-gp substrate, thus suffers from poor bioavailability (< 30%). The aim of this study was to develop and characterize LIN bioactive self-nanoemulsifying drug delivery system to circumvent its poor bioavailability and enhance its therapeutic efficacy.

Methodology

In this study, we developed solid supersaturated bioactive self-nanoemulsifying drug delivery system (Ss-bio-SNEDDS) of LIN, using clove oil as an oil phase, cremophor CO 40 as a surfactant, labrasol as a co-surfactant and Hydroxy-propyl-B-cyclodextrin (HPBCD) as a precipitation inhibitor (PI); all components are of established P-gp inhibition activity. Optimization was performed by means of triangular mixture design based on particle size, poly dispersity index (PDI) and percent transmittance. The two optimized formulations (F4 and F8) were designated and evaluated for stability and cloud point. Also, the effect of pH on particle size and PDI was assessed. Additionally, examination of particles' surface morphology of the two optimized formulations was performed by transmission electron microscope (TEM). The prepared liquid supersaturated-SNEDDS (s-SNEDDS) were converted into solid supersaturated-SNEDDS (Ss-SNEDDS) via adsorption on microcrystalline cellulose (MCC). Further evaluations were carried out, including in vitro drug release, in vitro precipitation and in vivo studies.

Results

The optimized formulations F4 and F8 manifested promising characteristics concerning particle size (< 50 nm), PDI (< 0.3) and percent transmittance (> 99%). Stability study showed no phase separation or precipitation with rapid emulsification time. The two optimized formulations showed high cloud point temperature (above 70°C). TEM images of F4 and F8 showed spheroid like appearance with relatively smooth surface. Results of the in vivo study in rats revealed a significant increase in AUC of supersaturated-F4, supersaturated-F8 and solid supersaturated-F4 (s-F4, s-F8 and Ss-F4) by 2.32, 2.89 and 2.54 folds, respectively compared to LIN solution; with a noticeable reduction in blood glucose level at each point.

Conclusion

In a nutshell, Ss-bio-SNEDDS are considered as auspicious nano-carriers for LIN with the virtue of augmented bioavailability and possible dose reduction.

Key words

Linagliptin, Supersaturation, Bio-SNEDDS, Clove oil, P-gp inhibition, Triangular mixture design.

Abbreviations

API	active pharmaceutical ingredients
LIN	Linagliptin
DPP-4	dipeptidyl peptidase 4
GIP	gastric inhibitory hormone
GLP-1	glucagon like peptide
P-gp	P-glycoprotein
Ss-bio-SNEDDS	solid supersaturated bioactive self-nanoemulsifying drug delivery system
HPBCD	Hydroxy-propyl-B-cyclodextrin
PI	precipitation inhibitor
PDI	poly dispersity index
AUC	Area under curve
GRAS	generally regarded as safe
SMEDDS	Self micro-emulsifying drug delivery system
s-SNEDDS	Supersaturated SNEDDS
Ss-SNEDDS	solid supersaturated self-nanoemulsifying drug delivery system
SLN	solid lipid nanoparticles
GIT	Gastro-intestinal tract
DAOI	designated area of interest
TEM	Transmission electron microscopy
FTIR	Fourier Transformed Infra-Red Spectroscopy
BGL	Blood glucose level

1. Introduction

Diabetes mellitus is a metabolic chronic disorder which occurs due to deficiency in insulin secretion, insulin action or both, resulting in high levels of blood glucose. Several oral antidiabetic drugs are available in the market such as biguanides, sulfonylureas and other classes. Weight gain and risk of hypoglycemia are the most common side effects accompanied with the administration of these drugs.

Dipeptidyl peptidase 4 (DPP-4) inhibitors are novel active pharmaceutical ingredients (API) for treatment of type II diabetes mellitus. Their action focuses on modulating the action of incretin hormone, gastric inhibitory hormone (GIP) and active glucagon like peptide (GLP-1) [1]. They have the advantages of lower risk of both hypoglycemia and weight gain over other treatments [1]. One of these drugs is linagliptin (LIN) (Fig. 1); which is considered as a potent selective oral DPP-4 inhibitor (with 80% inhibition over 24 hours) [1]. LIN was first approved in US, Europe and other countries in 2011 as single strength once daily dose of 5 mg [2]. It has been reported to be safe in geriatrics and patients with impaired renal functions.

Linagliptin is rapidly absorbed after oral administration achieving C_{max} at 90 minutes. Unfortunately, LIN is a P-glycoprotein (P-gp) substrate [3] thus, subjected to diminished oral bioavailability due to efflux in the G.I.T lumen. LIN is reported to be a BCS class III drug, so it has high solubility and low permeability. Its absolute bioavailability is approximately 30% and the remaining dose is excreted unchanged in urine and by liver [1,2].

Several techniques have been adopted to increase LIN bioavailability, like the incorporation into floating polymeric nanoparticles [4], solid lipid nanoparticles [5], SMEDDS [6], niosomes [7], eudragit coated sensitive SLN [8], as well as employment of natural phenols such as gallic and ellagic acid [9] and nanospsheres [10].

The purpose of this research was to apply nanotechnology as well as to employ P-gp modulators to improve the permeability of LIN [11]. The successful design of the system depended on maintaining the bioactive effects of the selected excipients as well as profiting their established P-gp inhibition activity. Additionally, self-emulsifying drug delivery systems (SEDDS) are reported to potentiate the inhibition activity of P-gp inhibitors through their delivery proximal to gut wall to exert their inhibitory effect [11, 12]. On the other hand, SEDDS can have ultrafine oil droplets (< 50 nm) which may be considered as a defense mechanism against enzymatic degradation and provide protection against identification by P-gp efflux transporter [11]. P-gp protein inhibition activity, solubilization of the drug and emulsification efficiency of surfactants are the main factors that govern choice of the system excipients.

Bioactive SNEDDS using natural oils have the merits of enhancing the bioavailability of the incorporated drug, and providing beneficial bioactive oils to patients [13]. The use of bioactive essential oils (which are GRAS (generally regarded as safe) by FDA) has several advantages such as availability, low cost and functionality as oil phases in the preparation of SNEDDS [11]. Furthermore, bioactive oils are capable of suppressing P-gp efflux transporter [11]. One of these oils is clove oil which is used as bioavailability enhancer based on its P-gp inhibition activity [14].

However, some impediments may encounter conventional liquid-SNEDDS such as drug precipitation following dilution in the GIT; which is believed to be a serious problem concerning the formulation of SNEDDS. To overcome this obstacle, water-soluble precipitation inhibitors (PIs) were used to yield supersaturated SNEDDS. The PIs delay the drug precipitation following dilution in the GIT and maintain a temporary supersaturated state [15]. Conventional

liquid-SNEDDS are incorporated in soft gelatin capsules; yet suffer drug leakage after prolonged storage; besides some incompatibilities between capsule and excipients may arise leading to instability problems [15, 16]. Solid carriers can overcome these glitches, where liquid-SNEDDS are adsorbed into solid carriers resulting in solid–SNEDDS which are more stable than liquid systems, accepted by patients and of low cost [15].

To date, no research has been published on utilization of SNEDDS along with excipients with proven P-gp inhibitory effect for enhancement of the permeability and bioavailability of linagliptin.

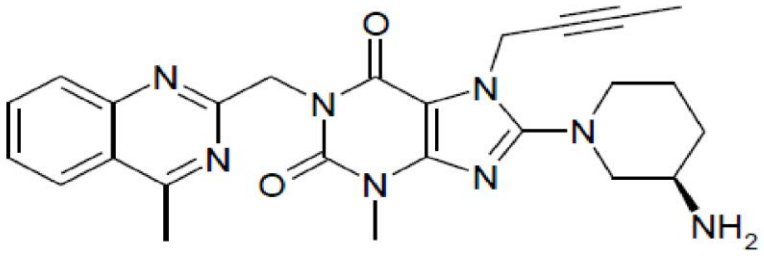

Fig. 1. Structure of linagliptin (LIN)

2. Materials and methods

2.1 Materials

Linagliptin (LIN) was obtained as a gift from Global Napi pharmaceuticals (GNP), Egypt. Clove oil, peppermint oil, linseed oil and cardamom oil were purchased from Alpha CHEM Co. (Egypt). Hydroxy propyl-B-cyclodextrin (HPBCD) was obtained from XI'AN HEALTH BIOCHEMICAL TECHNOLOGY CO., LTD. Labrasol was kindly donated by Gattefosse, France. Cremophor CO 40 CAS NO: 61788-85-0 was obtained from Pharmalog. Alloxan monohydrate CAS NO. 2244-11-3 was obtained from Alpha Chemica, India. Millipore filters (0.45 µm and 0.22 µm) were obtained from Cornell lab, Cairo, Egypt. Potassium dihydrogen orthophosphate and disodium hydrogen phosphate were obtained from El-Nasr Pharmaceutical Chemical Co., Cairo, Egypt. EMCOCEL LP 200 (MCC 200) and EMCOCEL LM 50 (MCC 50) CAS NO. 9004-34-6 were obtained from MENDELL, Uk. All other chemicals were of analytical grade.

2.2 Solubility of LIN in various oils, surfactants and co-surfactants

Solubility of LIN was scanned in different oils (linseed oil, clove oil, peppermint oil and cardamom oil), different surfactants (cremophor CO 40, PEG 400 and tween 20) and different co-surfactants (labrasol and transcutol) by using shake flask method. Excess amount of LIN was added to 2 ml of each vehicle. After sealing of the tubes, each mixture was vortexed by vortex mixer (CM 101, Remi, Mumbai, India) for 3 minutes for solubilization of the drug, then kept in shaking water bath (Grant instrument Cambridge Ltd., Barrington Cambridge, England) for 3 days at 37 ± 0.5ºC and 50 rpm to attain equiliribium. Subsequently, samples were centrifuged at 5000 rpm for 15 min; then, the supernatant was collected, filtered by 0.45 µm Millipore filter and finally the solubility was determined by measuring the absorbance at 228.5 nm after suitable dilution using UV spectrophotometer (SPD-20A UV-Vis detector) [17]. Solubility study was done in triplicate and the results were calculated as mean ± SD.

2.3 Emulsification efficiency and percent transmittance

Based on the solubility study, clove oil was chosen as the oil phase. Surfactants were chosen based on their ability to emulsify rather than solubilize the drug [18]. Also, oil- surfactant mixture should be able to solubilize the therapeutic dose of the drug [19]. Each surfactant (cremophor CO 40, PEG 400, tween 20) was mixed with the chosen oil phase (clove oil) in a ratio of 1:1. The effect of co-surfactant on emulsification was also studied; where the chosen surfactant (cremphor CO 40) was mixed with co-surfactants (either labrasol or transcutol) in a ratio of 2:1 and then surfactant mixture was mixed with clove oil in a ratio of 1:1. The mixtures were mixed by vortex mixer (CM 101, Remi, Mumbai, India) for 1 min; after that, 2 ml was taken from each mixture and diluted to 100 ml with distilled water. The ease of emulsion formation was recorded by the number of volumetric flask inversions required to produce a uniform dispersion and the self-emulsification was evaluated according to Table 1. The mixtures that showed the best emulsification were allowed to stand for 2 hours and clarity was evaluated by measuring % transmittance [20, 21, and 22]. Percent transmittance was measured using UV spectrophotometer (SPD-20A UV-Vis detector) at 638.2 nm after diluting 1 ml of the mixture to 100 ml with distilled water [21, 23].

Table 1 Grading system for evaluating self-emulsification efficiency [22, 23].

Visual observation	Aspect	Grade
Rapid nanoemulsion formation in < 1 min, which is clear and transparent, high spreadability.	Bluish tinge	A
Rapid nanoemulsion formation in < 2 min which is slightly less transparent, less clear.	Bluish white tinge	B
Milky emulsion formed within 2 min.	Milky white tinge	C
Dull grayish white emulsion, slow emulsification, with non-uniform distribution of oil droplets.	Dull white	D

2.4 Construction of ternary and pseudo-ternary phase diagrams

Ternary diagram was constructed to identify self-nanoemulsifying region. Based on the emulsification efficiency and percent transmittance, cremophor CO 40 was selected as the surfactant and labrasol was selected as co-surfactant. Self-emulsification ability was evaluated by diluting 1 ml of SNEDDS with 100 ml of distilled water; the obtained dispersion was allowed to stand for 2 hr and the percent transmittance was determined at 638.2 nm. Only clear or slightly bluish dispersions were considered to be in the nanoemulsion region of the diagram. Total sum of the three components in any mixture must add up to 100% [20].

The effect of LIN addition on the boundaries of the self-emulsifying region was also studied. Eight mixtures were prepared by using constant amount of drug (5 mg of LIN) as illustrated in Table 2 [24].

Table 2 Composition of the suggested SNEDDS loaded with LIN (boundaries of the self-emulsifying region)

Formulation code	Clove oil %	Cremophor CO 40 %	Labrasol %	Observation /grade	% Transmittance
C1	10	50	40	Clear / A	99.77 ± 0.11
C2	20	20	60	Clear / A	99.19 ± 0.11
C3	30	20	50	Clear / A	98.96 ± 0.12
C4	40	20	40	Clear / A	99.42 ± 0.11
C5	50	20	30	Clear/A	99.12 ± 0.28
C6	60	20	20	Clear/A	99.36 ± 0.28
C7	70	10	20	Clear/A	99.31 ± 0.27
C8	80	20	0	Clear/A	99.08 ± 0.23

2.5 Optimization of SNEDDS by triangular mixture design

Triangular mixture design is a novel customized screening method for selecting promising SNEDDS formulations with limited number of trials. The screening is based on a set of previously determined specifications. Herein, these specifications were customized to narrow droplet size (< 50 nm), low poly dispersity index value (PDI < 0.3) and high % transmittance (> 99%), in order to achieve higher stability and augmented bioavailability [25].

2.5.1 Triangular mixture design

Firstly, the center point of the triangle was confined and detected (F1); then, a hexagon was drawn around this center point (Fig.2). Only mixtures described by the vertices of the hexagon were analyzed. These vertices are designated as (F2, C4, F3, F4, F5 and C1) respectively. By analyzing the information obtained from the hexagon, further optimization was specified according to designated area of interest (DAOI) which is an area within the hexagon that manifested the aforementioned required specifications. This further optimization was done by using another geometric shape, which in this case, is trapezoid. The points representing the vertices of this trapezoid were analyzed to find out the optimized mixtures with the pre-set criteria required; Fig.2 illustrates the four vertices of the trapezoid (C3, C4, F4 and F8). All the selected SNEDDS representing the vertices of hexagon and trapezoid, in addition to the center point (F1) were analyzed with respect to droplet size, PDI and % transmittance.

2.5.2 Droplet size and PDI evaluation

Droplet size and PDI of the prepared nanoemulsions were measured by photon correlation spectroscopy (Zetasizer, Nano-ZA 90, Malvern, UK). One milliliter of each formulation was diluted up to 10 ml with deionized water and mixed gently with vortex mixer (CM 101, Remi, Mumbai, India), then particle size and PDI were determined [26]. Percent transmittance was measured as mentioned before.

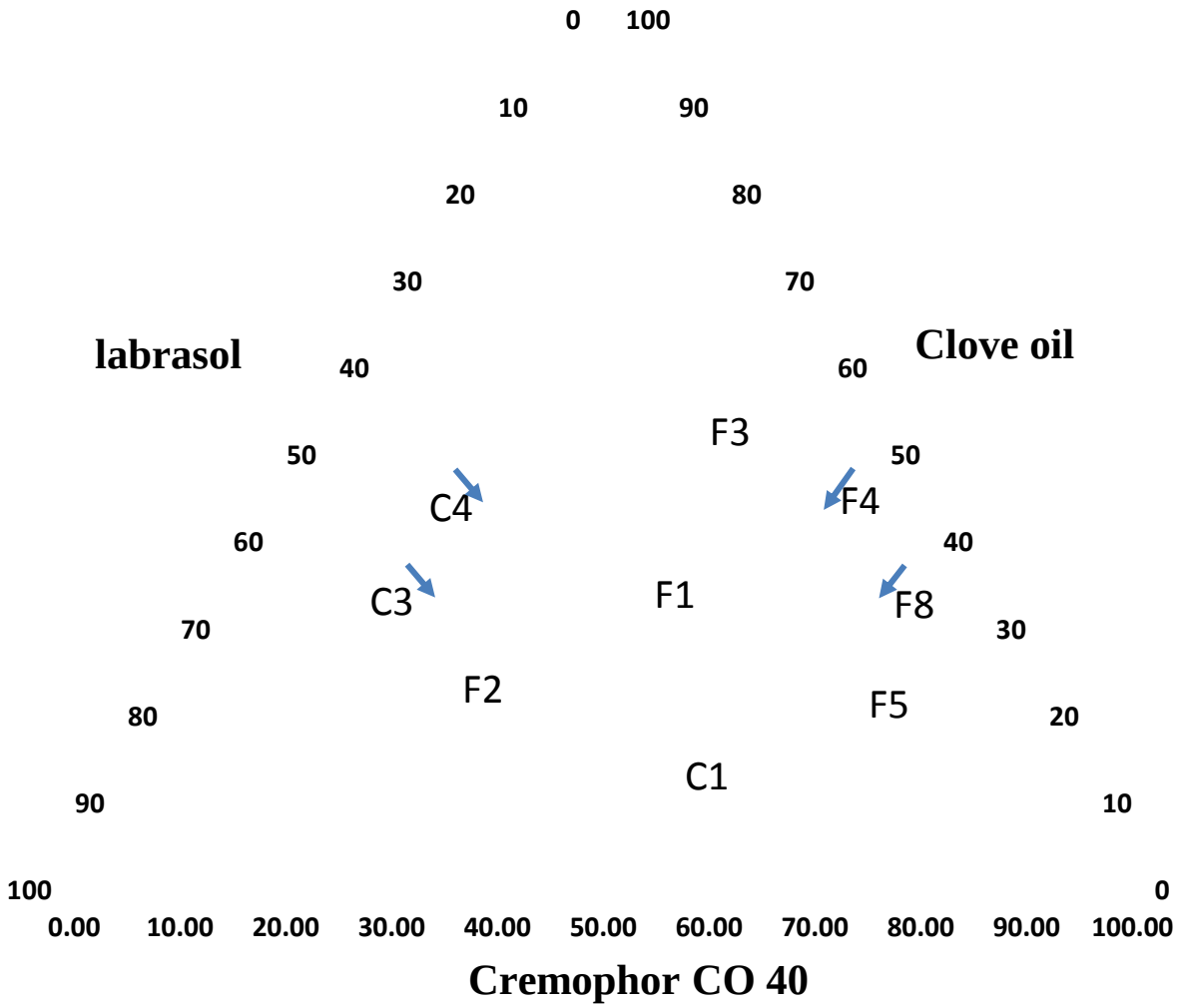

Fig. 2. Triangular mixture design representing DAOI. The green point represents the center point (F1); the black points represent the hexagon (F2, C4, F3, F4, F5, and C1) and the blue arrows represent the trapezoid structure (C3, C4, F4, and F8).

Based on the results obtained from optimization by triangular mixture design, F4 and F8 (with clove oil: cremophor CO 40: labrasol ratio of 40:50:10 and 30:60:10, respectively) were chosen for further evaluations.

2.6 Evaluation of optimized SNEDDS (F4 and F8)

2.6.1 Stability study

2.6.1.1 Robustness to dilution

Robustness to dilution is a key parameter in evaluating the stability of SNEDDS following high dilution in the G.I.T. One ml of each formulation (F4 and F8) was diluted with distilled water, 0.1 N HCL and phosphate buffer pH 7.4, each at a ratio of 1:50, 1: 100 and 1:1000. The diluted preparations were stored at ambient temperature for 24 hours and then observed for phase separation, clarity, precipitation and self-emulsification time. The experiment was done in triplicate [27, 15].

2.6.1.2 Thermodynamic stability study

Different stress conditions (centrifugation, heating-cooling and freeze-thaw stresses) were applied to F4 and F8 to evaluate thermodynamic stability.

2.6.1.2.1 Centrifugation study

The two optimized SNEDDS formulations (F4 and F8) were diluted with distilled water (1:25) and centrifuged at 5000 rpm for 30 mins [15]. F4 and F8 were checked for instability signs such as phase separation, creaming or cracking [27, 28].

2.6.1.2.2 Heating-cooling cycle

The testing procedure involves three cycles of storage at 4 ºC and 45 ºC for 48 hrs at each temperature. The formulations (F4 and F8) were checked for drug precipitation and phase separation, followed by dilution with distilled water (1:25) and the resulting nanoemulsions were observed for instability problems [15].

2.6.1.2.3 Freeze-thaw stress (accelerated aging)

The experiment involves freezing at - 4°C for 12 hrs then storing at 4°C for additional 12 hrs; both F4 and F8 were checked for instability signs [15, 29].

2.7 Characterization of the optimized SNEDDS (F4 and F8)

2.7.1 Cloud point measurement

Each formulation (F4 and F8) was diluted with distilled water (1:100) and placed in water bath with gradual increase in temperature. The temperature at which sudden appearance of cloudiness takes place is visually recorded and is considered as the cloud point [30].

2.7.2 Effect of pH change on particle size and PDI

Particle size and PDI of both optimized formulations were examined in different pH media to ensure stability of nanoemulsion. Measurements were assessed after tenfold dilution of samples with deionized water and 0.1N HCL (pH1.2), respectively [16].

2.7.3 Zeta potential

The zeta potential of the optimized formulations was measured using the Laser Doppler velocimetry technique of the zetasizer (Zetasizer, Nano-ZS 90, Malvern, UK). The diluted samples were put in an electrophoretic cell until a potential of 150 mV was established. The experiment was done in triplicate as mean ± SD [28].

2.7.4 Transmission electron microscopy (TEM)

The surface morphology of the particles of the two optimized formulations was examined by transmission electron microscope (TEM) (JEM-2000EX II Electron Microscope, JEOL, LTD, Tokyo, Japan). Prior to examination, one ml of each formulation was diluted with deionized water 10 times until clear nanoemulsion is obtained. One drop of the nanoemulsion was placed on a copper grid with carbon film coat. The grid was air-dried at room temperature and then samples were examined by microscope [15].

2.8 In vitro release study and release kinetics

In vitro release study was done in dissolution apparatus II, paddle method (Abbota, USA) at 100 rpm at 37 ºC, using cellulose dialysis membrane (pore size 2.4 nm, MWCO 12 K–14 K Da,). The dialysis membrane was soaked in phosphate buffer pH 7.4 for 30 minutes and then rinsed thoroughly. Subsequently, 0.5 ml of either F4, F8 or an equivalent amount of LIN solution in phosphate buffer were loaded in the dialysis bags then, they were closed from both ends using membrane clips. The bags were immersed in 500 ml phosphate buffer pH 7.4 as a dissolution medium. Five ml aliquots were withdrawn at different time intervals, filtered with 0.45 µm filter paper and replenished by fresh medium. The absorbance was measured spectrophotometrically (SPD-20A UV-Vis detector) at 228.5 nm [7]. The experiment was performed in triplicate. The mechanism of LIN release was studied by fitting in vitro release data into different kinetic models.

2.9 Preparation of supersaturated SNEDDS (s-SNEDDS)

Supersaturated SNEDDS (s-SNEDDS) are thermodynamically stable systems that can accommodate high amount of drug without the risk of precipitation. Supersaturation can be induced by means of precipitation inhibitors (PIs) [31]. For preparation of s-SNEDDS, different percentages of HPBCD (10, 15 and 25 % (w/w)) were added to each of the two optimized formulations (F4 and F8) and mixed using vortex mixer (CM 101, Remi, Mumbai, India) to get uniform solutions. Drug loaded samples (without addition of the HPBCD) were prepared for comparison [31].

2.10 In vitro precipitation study

In vitro precipitation test was applied to evaluate the performance of HPBCD as precipitation inhibitor. Half ml of SNEDDS (F4 and F8) as well as their supersaturated analogues (s-SNEDDS containing 10,15, 25% w/w of HPBCD) were added into dissolution apparatus II cells, each containing 200 ml of phosphate buffer pH 7.4 and operated at 100 rpm and temperature of 37 ºC. Two ml samples were withdrawn without replacement at 0.5, 1, 1.5, 2, 3 and 4 hrs, filtered by 0.22 µm filter paper and measured spectrophotometrically at 228.5 nm after suitable dilution with phosphate buffer [31]. Statistical analysis was performed by one way analysis of variance followed by Tukey-Kramer multiple comparisons test.

2.11 Characterization of s-SNEDDS

2.11.1 Viscosity measurement

F4 containing 15% HPBCD (s-F4) and F8 containing 25% HPBCD (s-F8) as precipitation inhibitor demonstrated the best apparent solubility and hence were chosen for further evaluations. The viscosities of SNEDDS (F4 and F8) and s-SNEDDS (s-F4 and s-F8) were evaluated by using MYR viscometer at 30 rpm and 25 ºC [23, 24].

2.12 Preparation of solid supersaturated –SNEDDS (Ss-SNEDDS)

The optimized supersaturated SNEDDS (s-SNEDDS) were converted to solid supersaturated-SNEDDS (Ss-SNEDDS) by adsorption onto solid carriers. One ml of each formulation (s-F4 and s-F8) was thoroughly mixed with a mixture of both MCC 50 and MCC 200 (with ratio of 1:1) to yield Ss-F4 and Ss-F8 in a free flowing powder form [21].

2.13 Characterization of Ss-SNEDDS

2.13.1 Fourier Transformed Infra-Red Spectroscopy (FTIR)

Infra-red spectra of linagliptin (LIN), MCC 50, MCC 200, solid formulations (S-F4, S- F8), solid supersaturated formulations (Ss-F4 and Ss-F8) and physical mixture containing LIN, HPBCD, and adsorbent mixture MCC50 and MCC200 (1:1) were examined by IR spectrophotometer (Thermo fisher scientific, Inc., Waltham, MA, USA) from 500 to 4000 cm^{-1} by using potassium bromide pellet technique [15].

2.13.2 Micromeritic properties of Ss–SNEDDS

2.13.2.1 Bulk and tapped density

To evaluate both bulk and tapped density, known amount of powder from each of Ss-F4 and Ss-F8 was taken into 10 ml measuring cylinder. The initial volume was estimated (bulk volume). After that, the cylinder was tapped against a hard surface at height of 2 cm several times until the volume was constant and the tapped volume was recorded.

Bulk Density (BD) = weight of the powder/Bulk volume.

Tapped Density (TD) = weight of the powder/Tapped volume.

2.13.2.2 Carr's Compressibility index and Hausner ratio

Carr's compressibility index was calculated according to the following equation:

Carr's compressibility index % = {(TD-BD)/TD} x 100 Eq. (1)

Hausner ratio is the ratio between tapped density and bulk density. It can describe the characters of powder particles.

Hausner ratio = TD/BD

2.13.2.3 Angle of repose (θ)

The angle of repose was calculated by funnel method. A funnel was fixed at constant height (2 cm) and a known amount of powder was allowed to fall on the edge of the funnel until the tip of the funnel touches the heap of the powder. Then, radius of the heap was recorded and angle of response was calculated according to the equation:

$\theta = \tan^{-1} h / r$ Eq. (2)

Where h is the height of the heap and r is the radius of the heap [24].

2.14 In vivo pharmacokinetic evaluation

2.14.1 Animals

Adult albino wistar rats (weighing about 250 gm) were obtained and located in cages for a week for accommodation with free access to food and water. Prior to experiment, the rats were fasted overnight with free access to water [32, 33].

2.14.2 Induction of diabetes

Single intraperitoneal injection of 150 mg/kg alloxan monohydrate (freshly prepared in normal saline) was adopted for induction of diabetes. Rats exhibiting elevation of fasting blood glucose level above 250 mg/dl at 72 hours post injection were considered diabetic and can be used for in vivo trials.

2.14.3 Experimental design

Diabetic rats were fasted 24 hrs prior to the experiment with free access to water. Animals were divided into five groups (five animals/group). Group 1 received blank SNEDDS as negative control. Group 2 received pure LIN in a dose of 3 mg/kg dispersed in 0.5 % W/V sodium CMC as positive control. Groups 3 and 4 received S-F4 and S-F8 (equivalent to 3 mg/kg of LIN). Group 5 received Ss-F4 (equivalent dose of 3 mg/kg of LIN) to demonstrate the effect of the PI (HPBCD) on LIN bioavailability. All formulations were administrated orally to animals by means of oral gavage. Blood samples were collected from the tail vein at different time intervals; then blood glucose level (mg/dl) of each sample was measured by using glucometer strip and accu-check device (Roche, San Francisco, CA).

Percent reduction in blood glucose level was calculated according to the following equation:

$$\text{Reduction in blood glucose level \% (RBGL)} = \frac{\text{BGL at } t_0 - \text{BGL at } t}{\text{BGL at } t_0} \times 100 \qquad \text{Eq. (3)}$$

Where percent reduction in blood glucose level represents the hypoglycemic response at each time interval. The area under percent reduction in BGL versus time curve was calculated.

2.15 Statistical analysis

Data were shown as mean ± SD and analyzed by (GraphPad software, INC., CA, USA).

Statistical analysis was performed by one way analysis of variance ($p < 0.05$) followed by Tukey-Kramer multiple comparisons test [34].

3. Results and Discussion

3.1 Solubility of LIN in various oils, surfactants and co-surfactants

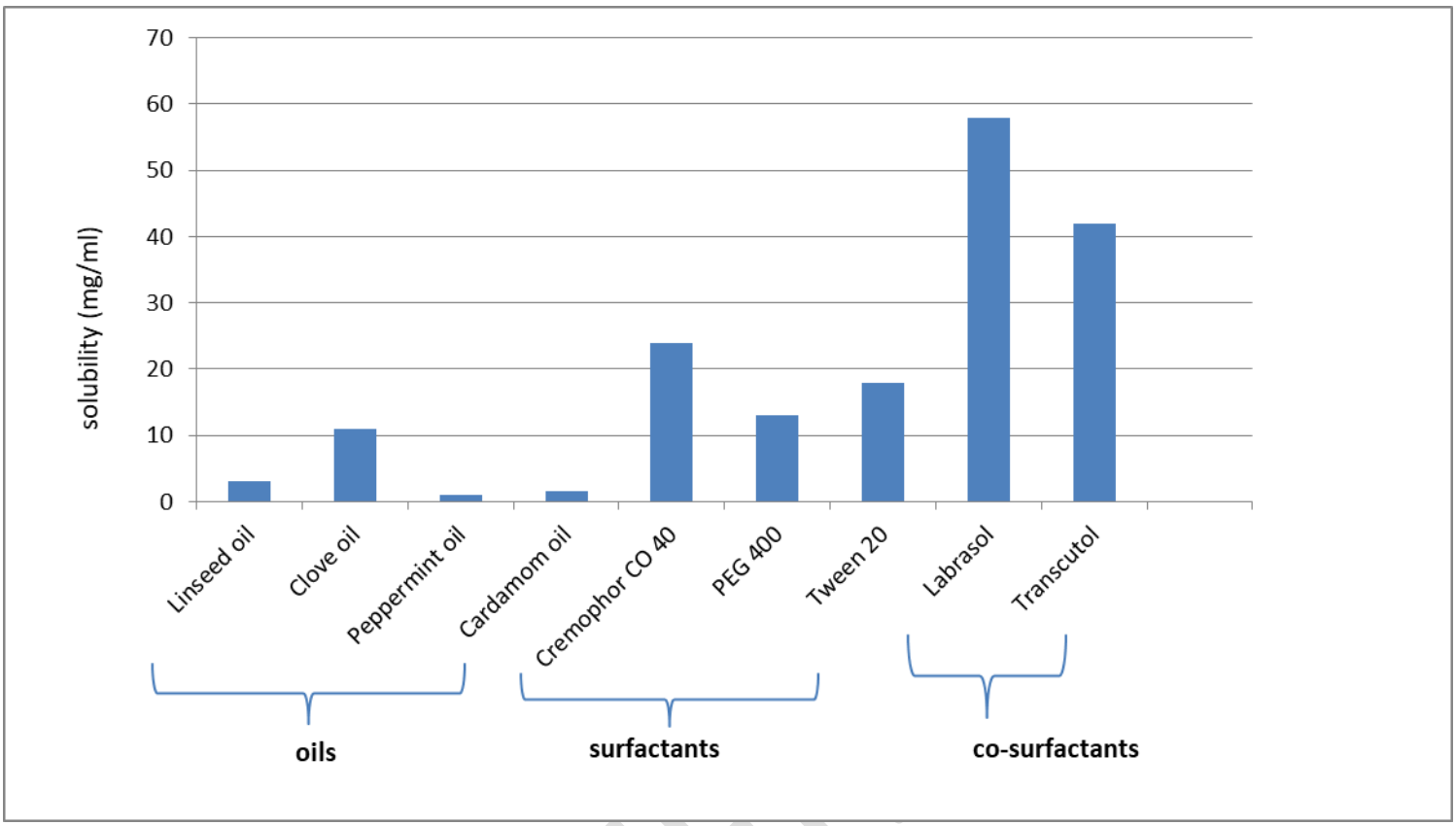

Fig. 3. Saturation solubility of LIN in various oils, surfactants and co-surfactants.

As depicted in Fig.3, LIN showed maximum solubility in clove oil, cremophor CO 40 as surfactant and labrasol as co-surfactant. Clove oil possesses also valuable effects in inhibiting microvascular and macrovascular complications of diabetes [35] and hence it was chosen as oil phase. Cremophor CO 40 was chosen as surfactant because of its superior effect in solubilizing LIN in addition to its ability to emulsify clove oil, as will be discussed later. Solubilization of LIN in SNEDDS excipients (clove oil, cremophor CO 40 and labrasol) is crucial for successful formulation to avoid drug precipitation before in situ emulsification in the gut [20]. Close scrutiny of Fig.3 divulges that solubility of LIN in the surfactant and co-surfactant is superior to the oil which may be ascribed to the intermediate partition coefficient of LIN (LogP = 1.7) [36]. Concerning surfactants, emulsification efficiency is the main factor in their choice; cremophor was reported to have excellent emulsification efficiency for essential oils [27]. Also, cremophor is known for its inhibition activity of both of P-gp and CYP3A4 [20, 21]. The choice of co-surfactant is dependent on its ability to solubilize the drug, its bioactive effects and safety, thus Labrasol was selected as a co-surfactant. Labrasol was reported to exert tight junction opening effect in low concentrations, thus improving intestinal absorption of many orally administered drugs [18, 21].

3.2 Emulsification efficiency and percent transmittance

Surfactant choice was motivated by assessment of emulsification efficiency which is based on % transmittance of the resulted nanoemulsion and number of flask inversions to obtain homogenous system. Mixture of clove oil and cremophor CO 40 required four inversions; while mixture of clove oil and PEG 400 required six inversions. Mixture of clove oil and tween 20 required more than ten inversions. Inversions less than five are reported to make good dispersion in water [21]. Cremophor CO 40 revealed the best emulsification ability (lowest number of inversions) and hence was chosen as surfactant. Cremophor, with high HLB (14-16), can result in better emulsification of the oil; the hydrophilicity of cremophor will eventually lead to rapid dispersion in G.I.T and formation of fine o/w emulsion [21]. Regarding co-surfactant choice, mixture of (Labrasol: cremophor CO 40) with clove oil required less number of inversions for nanoemulsion formation compared to transcutol mixture, hence Labrasol was designated as co-surfactant [20,21].

Percent transmittance plays an important role in evaluation of SNEDDS, where values close to 100% designate the nano size of the formed globules. This guarantees the ease of emulsification which is an important issue in the determination of rate and extent of drug release as well as drug absorption [29]. The percent transmittance of clove oil and cremophor CO 40 mixture (1:1) was 99.083%; while the surfactant mixture (cremophor: labrasol 2:1) with clove oil (1:1) showed a value of 98.401%.

3.3 Construction of ternary and pseudo-ternary diagrams

Ternary diagram was constructed to recognize the self-emulsifying region. Optical observation was the basis that determines self-emulsifying region where optical clarity with high % transmittance elucidates formation of SNEDDS. Also, the increase in the size of nanoemulsion region indicates better properties of the formed system [30]. Ternary phase diagram was constructed using distilled water in absence of LIN, where dark region indicates the formation of self-nanoemulsifying system (Fig. 4). On the other hand, pseudo ternary diagram, constructed in the presence of constant amount of LIN, showed no change in boundaries of the self-nanoemulsifying region.

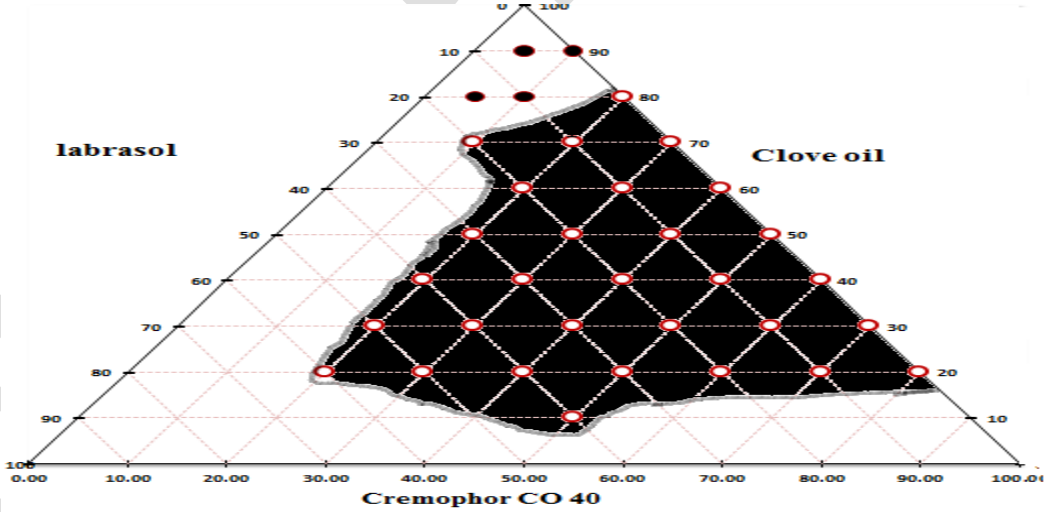

Fig. 4. Pseudo-ternary phase diagram using distilled water.

3.4 Optimization of SNEDDS by triangular mixture design

Triangular mixture design is a unique tool developed for optimization of SNEDDS [25], as it is time saving method with limited number of experiments; only 8-14 samples are analyzed instead of up to 50 samples on using traditional ways of optimization. The optimization process was based on choosing formulations which meet pre-set criteria (particle size < 50 nm, PDI < 0.3 and % transmittance > 99 %). These criteria are assumed to improve drug absorption leading to higher bioavailability. Droplet size is an important factor in evaluating SNEDDS in vivo, as the smaller the droplet size, the larger the interfacial area provided for drug diffusion, absorption and hence enhanced bioavailability. Also, droplet size is a key factor in determining the rate and amount of drug dissolved and absorbed in the G.I.T. The ultrafine droplet size of nanoemulsions (< 50 nm) makes the system robust to any apparent flocculation or coalescence; hence the system is kinetically stable with eventual rapid drug dissolution and release [20]. On the other hand, PDI values less than 0.3 warrant narrow size distribution of particles in the system [37] indicating high homogeneity of droplet size distribution. Table 3 illustrates particle size, PDI and percent transmittance of the center point as well as vertices of the hexagon. Based on the obtained results, trapezoid was chosen adjacent to F2, F3 and F5 of the hexagon. These three points showed particle size, PDI and percent transmittance close to the pre-set criteria required.

Table 3 Particle size, PDI and percent transmittance of mixture ratios representing vertices of hexagon structure

Formulation code	Mixture ratio (Clove oil: Cremophor CO 40: Labrasol)	Particle size (nm)	PDI	% transmittance
F1 (center point)	33.33:33.33:33.33	107.13 ±15.67	0.359 ± 0.003	99.54 ± 0.22
F2	20:30:50	20.22 ± 0.69	0.323 ± 0.012	99.57± 0.2
C4	40:20:40	19.72 ± 0.3	0.389 ± 0.029	99.42 ± 0.11
F3	50:30:20	52.7 ± 0.35	0.375 ±0.025	99. 65 ± 0.11
F4	40:50:10	17.73 ± 0.13	0.285 ± 0.063	99.77 ± 0.023
F5	20:60:20	16.76 ± 0.38	0.309 ± 0.003	99.36 ± 0.18
C1	10:50:40	91.72 ± 10.88	0.258 ± 0.002	99.77± 0.11

LIN amount was kept constant at 5 mg [a].

Table 4 Particle size, PDI and percent transmittance of mixture ratios representing vertices of trapezoid

Formulation code	Mixture ratio (Clove oil: Cremophor CO 40: Labrasol)	Particle size (nm)	PDI	% transmittance
C3	30:20:50	61.9 ± 1.47	0.260 ± 0.028	98.96 ± 0.12
C4	40:20:40	19.72 ± 0.3	0.389 ± 0.029	99.42 ± 0.11
F4	40:50:10	17.73 ± 0.13	0.285 ± 0.063	99.77 ± 0.023
F8	30:60:10	17.19 ± 1.23	0.284 ± 0.024	99.77 ± 0.11

LIN amount was kept constant at 5 mg [b].

As illustrated in Table 4, both F4 and F8 showed particle size < 50 nm, PDI < 0.3 and percent transmittance > 99%, thus were chosen for further evaluations.

3.5 Evaluation of optimized SNEDDS (F4 and F8)

3.5.1 Stability study

3.5.1.1 Robustness to dilution

Diluted SNEDDS (F4 and F8) yielded clear nanoemulsion in less than 30 seconds with no phase separation or precipitation at all tested dilutions in different media after 24 hours, which confirms the stability of the formed systems. Notably, precipitation of drug in vivo after dilution in the G.I.T will affect drug absorption and retard it [16]. After 24 hrs, following different dilutions folds in acidic medium, few crystals were observed. The appearance of those crystals may be attributed to significant separation of the hydrophilic surfactant from oil phase after acidic dilution [20]; accordingly, lower overall solubility of LIN in the diluted formulation. No crystals were observed neither in distilled water nor in phosphate buffer. This can be attributed to high stability of LIN in basic medium compared to acidic medium [36].

3.5.1.2 Thermodynamic stability study

No drug precipitation, creaming or phase separation were observed after subjecting the optimized SNEDDS (F4 and F8) to the stress conditions mentioned before (centrifugation, heating-cooling and freeze-thaw stresses). Clear transulant solution upon dilution of SNEDDS without any signs of phase separation or drug precipitation indicated the formulations stability and robustness to dilution. SNEDDS preconcentrates should have considerable stability to prevent drug precipitation, creaming or phase separation of the resulting nanoemulsion [20].

3.6 Characterization of the optimized SNEDDS (F4 and F8)

3.6.1 Cloud point measurement

Cloud point is the temperature above which nanoemulsion become cloudy. It occurs due to the dehydration of polyethylene oxide chains of non-ionic surfactants with consequent decrease in HLB values [20]. Cloud point above body temperature insured lack of phase separation in GIT [20]. Both F4 and F8 have a cloud point above 70ºC, which is much higher than body temperature, insuring stability of the formed nanoemulsion with no phase separation.

3.6.2 Effect of pH on particle size and PDI

Gastro intestinal tract has different pH ranges from acidic to basic. Particle size of the SNEDDS following dilution in the G.I.T should not change significantly over this PH range to ensure stability of the formed nanoemulsion. Table 5 clarifies that pH alteration did not influence the particle size and PDI in both F4 and F8, which means consistent dispersion of the formulation regardless the pH of the medium [16].

Table 5 Effect of pH on droplet size and PDI

Formulation	Particle size (nm)		PDI	
	Deionized water	0.1 N HCL	Deionized water	0.1 N HCL
F4	17.73 ± 0.13	16.51 ± 0.12	0.285 ± 0.063	0.224 ± 0.05
F8	17.19 ± 1.23	24.68 ± 3.4	0.284 ± 0.024	0.254 ±0.03

Data represented as mean value ± SD (n=3) [c].

3.6.3 Zeta potential

Zeta potential is an indication of stability of the formed nanoemulsion. F4 and F8 showed zeta potential values of -16.16 ± 2.1mV and -21.93 ± 1.56 mV respectively. The negative charge of the nanoemulsion droplets was probably due to ionization of the free fatty acids present in cremophor and labrasol [34]. This negative charge may have an advantage relative to permeability of the drug as GI epithelium is covered with mucus thin layer which act as defense mechanism against xenobiotics and pathogens but also hinders nanoparticles from passage through GIT. Though this mucus layer has negative charged structure, made of sulfonic and sialic acid, which acts as a barrier to positively charged nanoparticles (due to electrostatic interactions); it facilitates permeation of negatively charged nanoparticles [38, 39]. Additionally, cremophor as non ionic surfactant can enhance stabilization by steric repulsion [5].

3.6.4 Transmission electron microscopy (TEM)

The images for F4 and F8 are depicted in Fig. 5. The images showed the spheroid like appearance for F4 and F8 with relatively smooth surface. The droplet size ranged from 7 to 18 nm for F4 and from 3 to 14.4 nm for F8. It was reported that small nanoparticles are more suitable for cellular internalization via endocytosis, so F4 and F8 with size < 20 nm can enhance internalization of intestinal epithelial cell [40]. Also, the appearance of distinct non aggregated particles of nano emulsion indicates the physical stability of the prepared system [37].

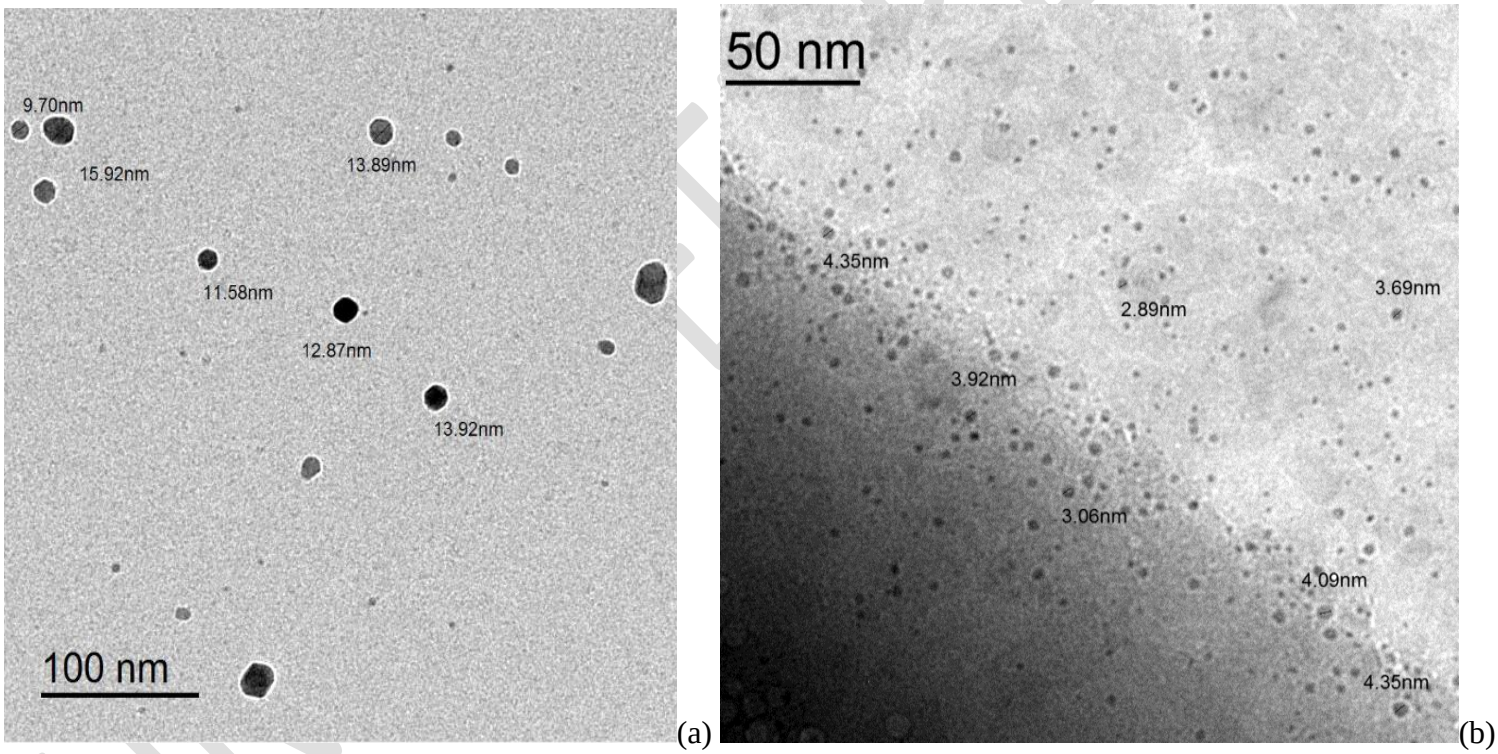

Fig. 5. TEM of formulations (a) F4 and (b) F8.

3.7 In vitro release study and release kinetics

The simulated release of LIN solution and optimized formulations (F4 and F8) was depicted in (Fig.6). The figure demonstrated apparent enhancement of drug release for both F4 and F8 compared to LIN solution. This may be ascribed to the small particle size and enhancement of drug solubility [6]. Both F4 and F8 demonstrated initial burst release compared to LIN solution. This phenomenon can be elucidated by means of surface associated drug, small

particle size of the nanodroplets formed and high surface area. This initial fast release was followed by slower sustained release pattern, which may be attributed to controlled diffusion of the drug from the nanoparticles [41].

The resulted data of both optimized formulations (F4 and F8) were fitted to different kinetic models such as zero order, first order, Higuchi and Korsermeyer-Peppas models to comprehend the kinetics of release. Table 6 illustrates the correlation coefficient (r^2) of each model. The Higuchi model demonstrated the best correlation. This could indicate that the release of LIN was predominantly by diffusion from oil droplets in sustained mode. Also, further confirmation of the exact mechanism of the drug release was performed by Korsermeyer-Peppas model.The release exponent (*n*) value for F4 was 0.7940 and 0.6360 for F8. Value of exponent (*n*) between 0.45 and 0.89 indicated non-Fickian (anomalous) release mechanism, including both erosion and diffusion [33].

Table 6 The calculated Correlation coefficients for the in vitro release of LIN from the optimized SNEDDS formulations representing different kinetic models

Formulation	Correlation coefficients (r^2)			
	Zero order	First order	Higuchi model	Korsermeyer-Peppas model
F4	0.7567	0.7492	0.8766	0.8654
F8	0.8158	0.7856	0.9054	0.8204

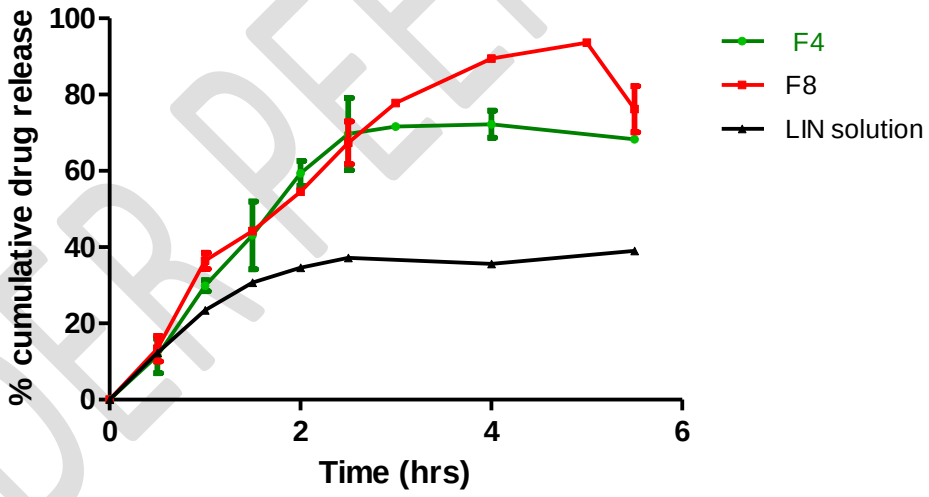

Fig. 6. In vitro release pattern of F4, F8 and LIN solution in phosphate buffer pH (7.4).

3.8 In vitro precipitation study

SNEDDS are exposed to dilution in the GIT; consequently drug precipitation can be induced following dilution in case of formulations accommodating high load of drug, thus these systems are considered thermodynamically unstable. Precipitation inhibitors can enhance thermodynamic activity by exceeding the apparent solubility of the drug, leading to elevation of free drug concentration with more affinity to cross biological barriers and more enhanced effect on the uptake reflux. Non polymeric precipitation inhibitors such as cyclodextrins (CDs) were proven

to decrease nucleation rate and crystal growth [42]. Also, previous studies concluded that CDs can enhance drug saturation solubility and can form hydrogen bond with the drug, thus inhibiting precipitation thermodynamically and kinetically, respectively. CDs also can achieve both springe and parachute effect; where hydrogen bonds can hinder the crystal lattice formation and as a consequence decrease the rate of crystal growth [43]. HPBCD as PI was reported to enhance bioavailability and inhibit precipitation of several drugs [43, 44]. On the other hand, HPBCD was proven to inhibit Pgp ATPase thus improve not only solubility but also permeability of p gp substrates [45].

In vitro precipitation under non sink conditions was performed to evaluate both the possibility of the drug to precipitate after dilution with aqueous medium and the degree of supersaturation. As depicted in Fig.7, different concentrations of HPBCD were evaluated. Only F4 containing 15% HPBCD manifested parachute effect of HPBCD in comparison to F4. F8 containing 25% HPBCD exhibited slower precipitation of LIN when compared to F8 ($p < 0.05$). On the other hand, the higher solubility profile of F4 containing 15% HPBCD and F8 containing 25% HPBCD compared to those of F4 and F8, respectively illustrates the spring effect (higher solubility) due to HPBCD. Hence, F4 containing 15% HPBCD (s-F4) and F8 containing 25% HPBCD (s-F8) were chosen for further studies. Also, the area under concentration time curve (AUC) revealed more precise evaluation of supersaturation, where the AUC for s-F4 was 2.53 fold higher than that of F4 and s-F8 was 1.33 fold higher than that of F8. Notably, supersaturation was sustained for over 120 minutes for both formulations [46].

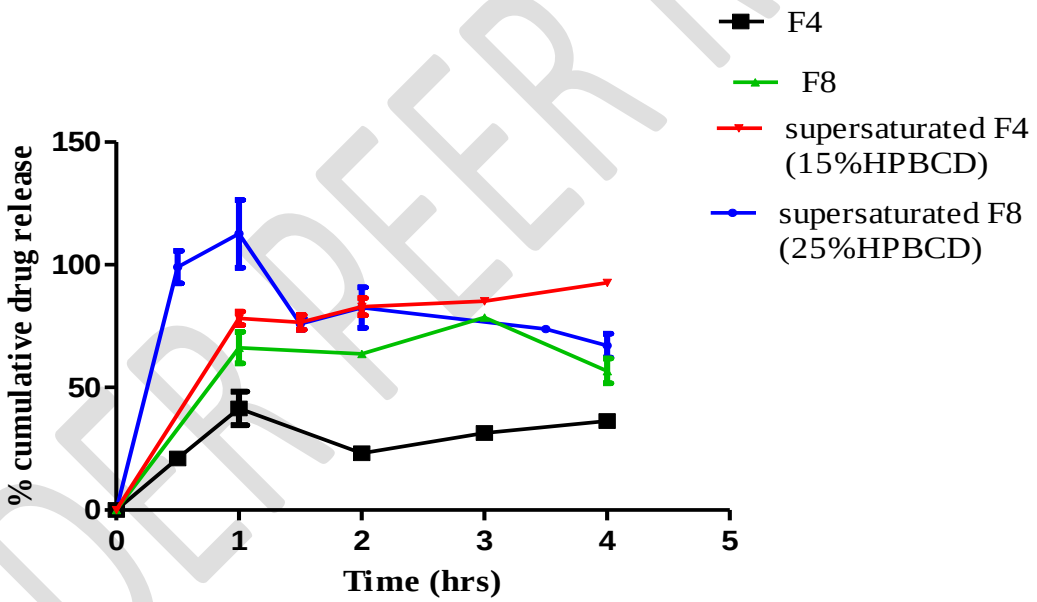

Fig. 7. Effect of HPBCD as PI on the apparent solubility of LIN from supersaturated-SNEDDS in phosphate buffer (pH 7.4).

3.9 Characterization of s-SNEDDS

3.9.1 Viscosity measurement

Systems with low viscosities can leak when filled into capsules; also highly viscous ones are hardly filled into capsules. Moderate viscous systems (between 0.1-1 Pa.s at 25 ºC) are most appropriate to be filled into capsules [47]. Both F4 and F8 demonstrated moderate viscosity values of 0.23 and 0.36 Pa.s, respectively. Conversely, supersaturated formulations showed a significant increase in viscosity, where both s-F4 and s-F8 exhibited viscosity values of 0.71 and 0.87 Pa.s, respectively. This may be ascribed to the presence of 15% HPBCD within s-F4 and 25%HPBCD within s-F8 as PI. This elevation in viscosity can retard the drug precipitation via hindrance of drug molecule diffusion to the crystal nucleus which can maintain supersaturation state [48].

3.10 Characterization of Ss-SNEDDS

3.10.1 Fourier Transformed Infra-Red Spectroscopy (FTIR)

FTIR was performed to detect the possibility of any interaction among the system components. As shown in Fig.8, FTIR spectrum of LIN demonstrated characteristic absorption peaks at 1348 and 1401 cm^{-1} representing axial deformation of aromatic tertiary amine. Quinazoline cluster was shown at 1519 cm^{-1}. Besides, both peaks depicted at 1658 and 1702 cm^{-1} revealed carbonyl in purine ring. Moreover, peaks located at 2833 and 2929cm^{-1} represent primary amine. Stretching of the N-H piperidine was represented by the peak at 3374 cm^{-1} (Fig.8 a) [49, 5]. Fig. 8d demonstrated no significant difference in the FTIR spectrum of the physical mixture compared to that of LIN. This emphasizes the absence of possible interaction between the drug and the adsorbants [15].

Peak representing N-H piperidine stretching was red-shifted to 3338 and 3339 cm^{-1} for solid supersaturated formulations (Ss-F4 and Ss-F8) (Fig. 8 h, g) in comparison to solid formulations (S-F4 and S-F8) respectively (Fig. 8 e, f). The strength and broadening of the N-H peak for both Ss-F4 and Ss-F8 may be due to formation of hydrogen bonding between HPBCD as PI and LIN [48].

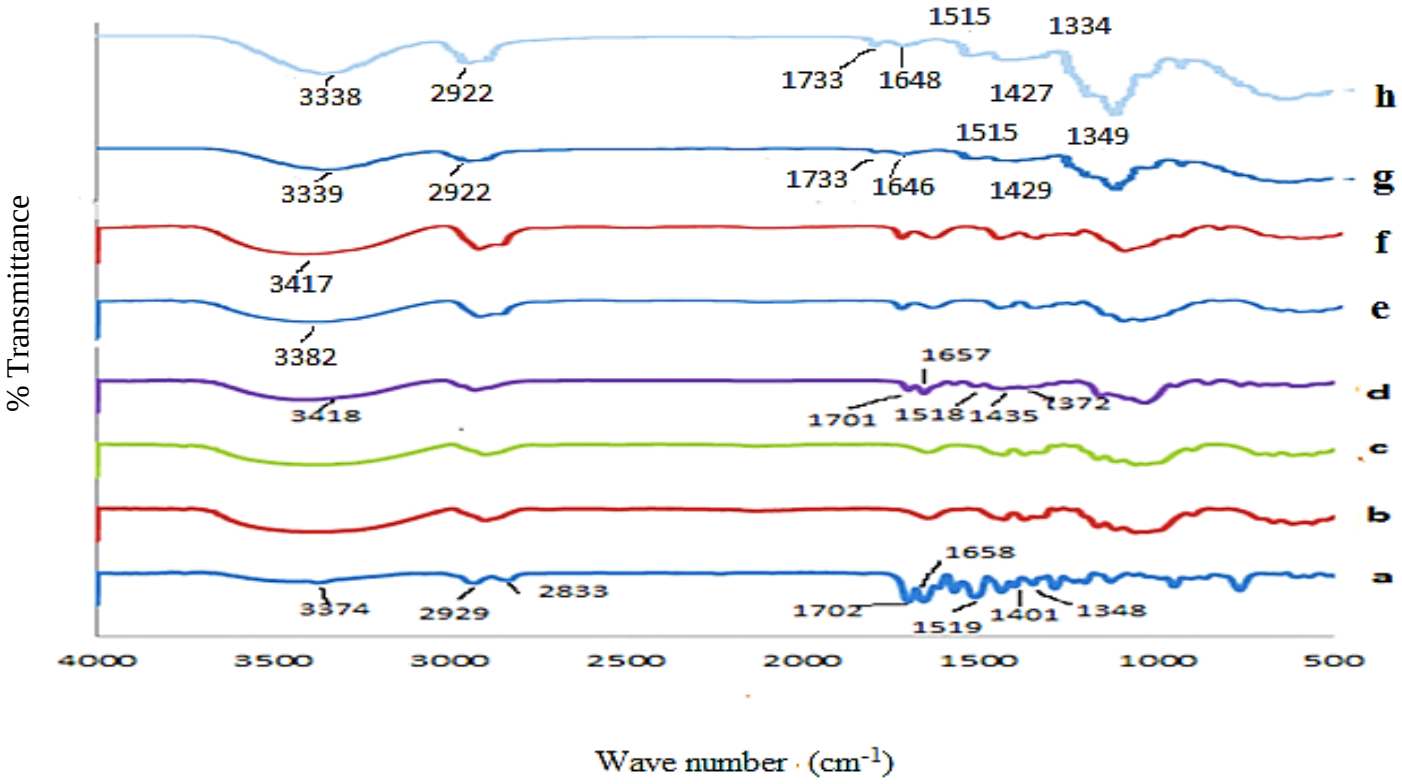

Fig.8. FTIR spectroscopy of (a) LIN, (b) MCC 50, (C) MCC 200, (d) physical mixture, (e) S-F4, (f) S-F8, (g) Ss-F8 and (h) Ss- F4.

3.10.2 Micromeritic properties of Ss–SNEDDS

Results of Carr's index, Hausner ratio and angle of repose are demonstrated in Table 7. Results revealed that both Ss-F4 and Ss-F8 have fair flow properties [24].

Table 7 Micromeritic properties of Ss-SNEDDS

Formulation	Carr's index %	Hausner ratio	Angle of repose	Flow properties
Ss- F4	13.199	1.15	36	Fair
Ss-F8	19.03	1.235	41	Fair

3.11 In vivo pharmacokinetic evaluation

Alloxan monohydrate was used to induce diabetes in rats. It reduces insulin secretion by generating free radicals that destroy islets of Langerhans resulting in hyperglycemia. The hypoglycemic effect of LIN was represented by measuring the percent reduction in blood glucose level as depicted in (Fig. 9). Careful examination of the figure reveals that, Group 3 (receiving S- F4), group 4 (receiving S-F8) and group 5 (receiving Ss-F4) showed significant ($p<0.05$) higher mean % reduction in BGL compared to group 2 (receiving LIN solution). On the other hand, the AUC for S-F4, S-F8 and Ss-F4 was 2.32, 2.89 and 2.54 folds higher than that of LIN solution, respectively; indicating a much higher reduction in BGL over 24 hrs for S-F4, S-F8 and Ss-F4, respectively. The lower AUC value for LIN solution was attributed to its low permeability mediated by P-gp efflux transport. On the other hand, the higher AUC

for S-F4, S-F8 and Ss-F8 was explained by the enhanced LIN permeation due to the inhibition of P-gp mediated transport. The incorporation of P-gp inhibitors (clove oil, cremophor CO 40 and labrasol) enhanced the permeability of LIN. The AUC of Ss-F4 was 1.09 folds higher than that of S-F4 due to incorporation of HPBCD; where HPBCD served as precipitation inhibitor in addition to its permeability enhancement effect, which improved LIN bioavailability. Additionally, the nanometric size of the SNEDDS particles facilitates their intact endocytosis and eventually satisfies enhanced bioavailability. It's worthy to mention that the reduction of BGL of S-F4, S –F8 and Ss-F4 was significant at each point in comparison with LIN solution [5].

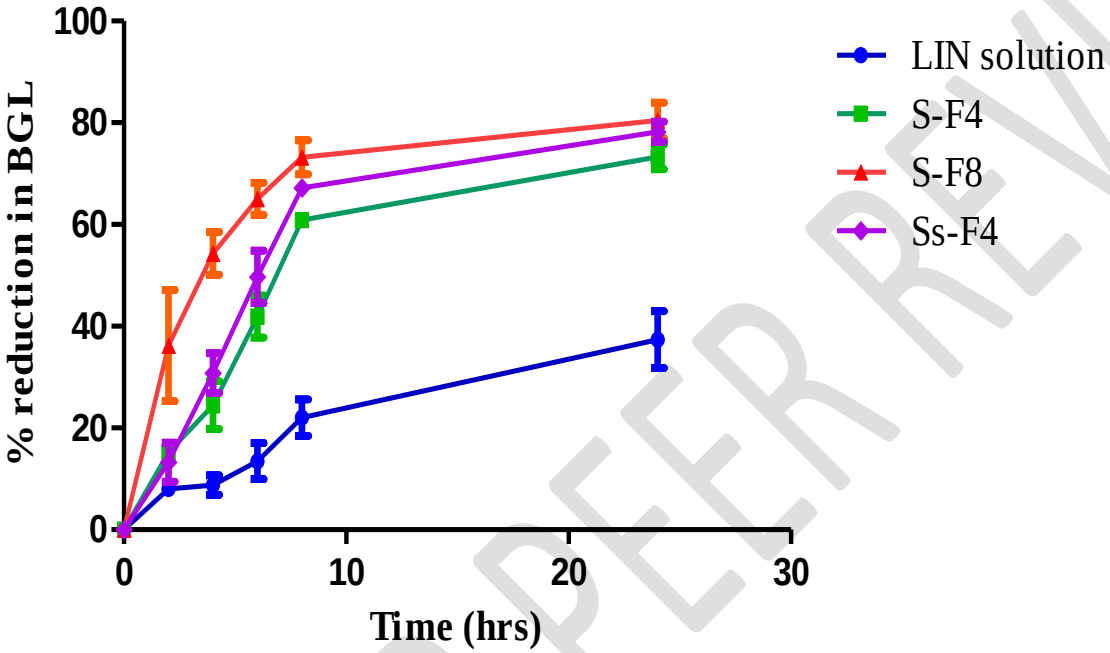

Fig. 9. In vivo reduction of BGL following oral administration of S-F4, S-F8 and Ss-F4 versus LIN solution in rats.

4. Conclusion

Linagliptin bio-SNEDDS were successfully developed, formulated and optimized using triangular mixture design based on predetermined criteria. The two optimized formulations showed particle size < 50 nm, PDI< 0.3 and % transmittance > 99%. Notably, the in vitro release study demonstrated an enhancement of the linagliptin release from F4 and F8. In vitro precipitation study involving the addition of HPBCD (PI and permeability enhancer) revealed lower precipitation of the drug as well as enhanced permeability with prospective enhancement of LIN solubility. Furthermore, the optimized SNEDDS formulations of LIN were converted to Ss-SNEDDS formulations with the purpose of enhancement of product design in addition to ease of preparation. The in vivo pharmacokinetic study revealed reduction of blood glucose level in rats, permeability enhancement and boosted bioavailability of the prepared bio-SNEDDS compared to LIN solution. Proper selection of the system components (clove oil, cremophor CO 40 and labrasol) with proven P-gp inhibition activity, in addition to HPBCD as PI has contributed to the desired

outcome. Furthermore, eventual dose reduction can be expected. In conclusion, development of Ss-bio-SNEDDS might be a promising platform for improving the bioavailability of linagliptin as well as other P-gp substrate drugs.

Ethical Approval:

All procedures were carried out according to guidelines of "Principals of laboratory animal care" (National institute of Health Publication No.85-23, revised 1985) after approval of ethical committee, Mansoura University, Egypt (Ethical approval code 2022-225). Furthermore, ARRIVE principals were applied to this study.

References

1. Scott L.J. Linagliptin: in type 2 diabetes mellitus. Drugs (2011); 71 (5): 611-624; http: // doi.org/ 10.2165/11207400.
2. Graefe-Mody U, Retlich S, Friedrich C. Clinical Pharmacokinetics and Pharmacodynamics of Linagliptin. Clin. Pharmacokinet (2012); 51 (7): 411-427; http: //doi.org/10.2165/11630900.
3. Park JW, Kim JM, Noh JH, Kim KA, Chung H, Kim E , et al. Pharmacokinetics of a Fixed-Dose Combination Product of Dapagliflozin and Linagliptin and Its Comparison With Co-Administration of Individual Tablets in Healthy Humans. Pharmaceutics (2022), 14, 591; DOI: 10.3390 /pharmaceutics14030591.
4. Prasanthi D, Kumari JK, Hymavathi S. Formulation and Evaluation of Floating Polymeric Nanoparticles of Linagliptin in Capsules. J Young Pharm (2020) 12 (2) Suppl: s32-s38.
5. Shah P, Chavda K, Vyas B, Patel S. Formulation development of linagliptin solid lipid nanoparticles for oral bioavailability enhancement: role of P-gp inhibition. Drug Deliv. and Transl. Res (2020); DOI: 10.1007/s13346-020-00839-9.
6. Patel MM, Patel RJ. Linagliptin loaded Solid-SMEEDS for enhanced solubility and dissolution: Formulation development and optimization by D-optimal design, J. Drug Deliv. & Therapeutics (2019) 9(2):47-56; http://dx.doi.org/10.22270/jddt.v9i2.2465.
7. Nishu SBN , Karmoker JR, Ali FF, Rafa NN, Hoque O, Dewan I. In vitro and Ex vivo Studies of Linagliptin Loaded Non-Ionic Surfactant Vesicles Using Statistical Optimization. Journal of Advances in Medical and Pharmaceutical Sciences (2018)18(2):1-16; DOI: 10.9734/JAMPS/2018/44198.
8. Veni DK, Gupta NV. Development and evaluation of Eudragit coated environmental sensitive solid lipid nanoparticles using central composite design module for enhancement of oral bioavailability of linagliptin. International Journal of Polymeric Materials and Polymeric Biomaterials (2019); DOI: 10.1080/00914037.2019.1570513.
9. Shaik M, Vanapatla SR. Enhanced oral bioavailability of linagliptin by the influence of gallic acid and ellagic acid in male Wistar albino rats: involvement of p-glycoprotein inhibition. Drug Metabolism and Personalized Therapy (2019); DOI: 10.1515/dmpt-2018-0020.
10. Nishitha A, Kumar AA. Formulation and Evaluation of Linagliptin Nanospheres. J. Pharm. Sci. & Res. Vol. 13(5), 2021, 288-293. https://www.jpsr.pharmainfo.in/Documents/Volumes/vol13issue05/jpsr13052109.pdf
11. Aboulfotouh K, Allam AA, EL-Badry M, EL-sayed AM. Self-emulsifying drug–delivery systems modulate P-glycoprotein activity: role of excipients and formulation aspects. Nanomed., 2018, vol. 13, NO. 14; http: //doi.org/10.2217/nnm-2017-0354.

12. Dash RN, Habibuddin M, Humaira T, Ramesh D. Design, optimization, and evaluation of glipizide solid self-nanoemulsifying drug delivery for enhanced solubility and dissolution. Saudi pharmaceutical journal (2015) 23,528-540; http://dx.doi.org/10.1016/ j.jsps.2015.01.0.
13. Kazi M, Shahba AA, Alrashoud S, Alwadei M, Sherif AY, Alanazi FK . Bioactive Self-Nanoemulsifying Drug Delivery Systems (Bio-SNEDDS) for Combined Oral Delivery of Curcumin and Piperine. Molecules (2020) 25, 1703; doi: 10.3390/molecules25071703.
14. Akhtar N, Ahad A, Khar RK, Jaggi M, Aqil M, Iqbal Z, et al. The emerging role of P-glycoprotein inhibitors in drug delivery: a patent review. Expert opin. Ther. patents (2011) 21(4): 561-576; DOI: 10.1517/ 13543776.2011. 561784.
15. Motawea A, Borg T, Tarshouby T, Abd EL-Gawad AH. Nanoemulsifying drug delivery system to improve the bioavailability of piroxicam. Pharmaceutical Development and Technology (2017) ISSN: 1083-7450 (Print) 1097-9867; http://dx.doi.org/10.1080/10837450.2016.1231810.
16. Alghananim A, ÖzalpY , Mesut B, Serakinci N, Özsoy Y and ungor SG. Solid Ultra Fine Self-Nanoemulsifying Drug Delivery System (S-SNEDDS) of Deferasirox for Improved Solubility: Optimization, Characterization, and In Vitro Cytotoxicity Studies. Pharmaceuticals (2020)13, 162; DOI: 10.3390/ph13080162(8), 162.
17. Alothaid H, Aldughaim MS, Yusuf AO, U. Yezdani, Alhazmi A, Habibullah M, et al. A comprehensive study of the basic formulation of supersaturated self-nanoemulsfying drug delivery systems (SNEDDS) of albendazolum. Drug deliv., (2021) 28:1, 2119-2126; DOI: 10.1080/10717544.2021.1986601.
18. Basalious EB, Shawky N, Badr- Eldin SM. SNEDDS containing bioenhancers for improvement of dissolution and oral absorption of lacidipine. I: development and optimization. Int. J. Pharm., 391 (2010) 203–211; DOI:10.1016/j.ijpharm.2010.03.008.
19. Taha EI, Al-Suwayeh SA, Tayel MM, Badran MM. Fast ultra-fine self –nanoemulsfying drug delivery system for improving in vitro gastric dissolution of poor water soluble drug. Acta Pol Pharma (2015) Vol. 72 No. 1 pp. 171-178. PMID: 25850213.
20. Aboulfotouh K, Allam AA, EL-Badry M, El-sayed AM. Development and in vitro/in vivo performance of self-nanoemulsfying drug delivery systems loaded with candesartan cilexetil. Eur. J. Pharm. Sci., 109 (2017) 503–513; http://dx.doi.org/10.1016/j.ejps.2017.09.001.
21. Patel G, Shelat P, Lalwani P. Statistical modeling, optimization and characterization of solid self-nanoemulsifying drug delivery system of lopinavir using design of experiment. Drug Deliv., (2016) 23 (8): 3027–3042; DOI: 10.3109/10717544.2016.1141260
22. Khan AW, Kotta S, Ansari SH, Sharma RK, Ali J. Self-nanoemulsifying drug delivery system (SNEDDS) of the poorly water-soluble grapefruit flavonoid Naringenin: design, characterization, in vitro and in vivo evaluation. Drug Deliv. (2014) 22:4, 552-561; DOI: 10.3109/10717544.2013.878003.
23. Bhagwat DA, Swami PA, Nadaf SJ, Choudhari PB, Kumbar VM, et al. Capsaicin loaded solid SNEDDS for enhanced bioavailability and anticancer activity: In-vitro, in-silico, and in-vivo characterization. Journal of Pharmaceutical Sciences (2020); DOI: https://doi.org/10.1016/j.xphs.2020.10.020.
24. Nasr AM, Gardouh AR, Ghonaim HM and Ghorab MM. Design, formulation and in-vitro characterization of Irbesartan solid self-nanoemulsifying drug delivery system (S-SNEDDS) prepared using spray drying technique. J. Chem. Pharm. Res.; (2016) 8(2):159-183. ISSN: 0975-7384.

25. Schmied FP, Bernhardt A, Engel A and Klein S. A customized Screening Tool Approach for the Development of a self-Nanoemulsfying Drug Delivery System (SNEDDS).AAPS pharmSciTech (2022) 23:39; DOI: 10.1208/s12249-021-02176-7.
26. Negi JS, Chattopadhyay P, Sharma AK, Ram V. Development of solid lipid nanoparticles (SLNs) of lopinavir using hot self nano-emulsification (SNE) technique. European Journal of Pharmaceutical Sciences (2013), Volume 48, Issues 1–2; http://dx.doi.org/10.1016/j.ejps.2012.10.022
27. Ali HSM, Ahmed SA, Alqurshi AA, ALalawi AM, Shehata AM and AlahmadiYM. Tadalafil- loaded Self-Nanoemulsfying Chewable Tablets for improved Bioavailability:Design, In Vitro, and In Vivo Testing. Pharmaceutics (2022) 14, 1927; https://doi.org/10.3390/pharmaceutics14091927.
28. Ujilestari T, Martien R, Ariyadi B, NaDono ND, Zuprizal. Self-nanoemulsifying drug delivery system (SNEDDS) of Amomum compactum essential oil: Design, formulation, and characterization. Journal of Applied Pharmaceutical Science (2018) Vol. 8 (06), pp 014-021; DOI: 10.7324/JAPS.2018.8603.
29. Rathore C, Hemrajani C, Sharma AK, Gupta PK, Jha NK, Aljabali AAA, et al. Self-nanoemulsifying drug delivery system (SNEDDS) mediated improved oral bioavailability of thymoquinone :optimization, characterization, pharmacokinetic, and hepatotoxicity studies. Drug delivery and Translational Research (2022); **https://doi.org/10.1007/s13346-022-01193-8**.
30. Ke Z, Hou X, Jia XB. Design and optimization of self-nanoemulsifying drug delivery systems for improved bioavailability of cyclovirobuxine D. Drug Design, Development and Therapy (2016). 10: 2049–2060; DOI:10.2147/DDDT.S106356.
31. ELkasabgy NA. Ocular supersaturated self-nanoemulsifying drug delivery systems (S-SNEDDS) to enhance econazole nitrate bioavailability. International Journal of Pharmaceutics 460 (2014) 33–44; http://dx.doi.org/10.1016/j.ijpharm.2013.10.044.
32. Momoh MA, Kenechukwu FC, Attama AA. Formulation and evaluation of novel solid lipid microparticles as a sustained release system for the delivery of metformin hydrochloride. Drug Deliv, (2013) 20:3-4,102-111; DOI: 10.3109/10717544.2013.779329.
33. Mohsen AM, Abousamra MA, ELshebeiney SA. Enhanced Oral bioavailability and sustained Delivery of Glimepiride via Niosomal Encapsulation: In-vitro Characterization and In-vivo Evaluation. Drug Development and Industrial pharmacy (2017); ISSN: 0363-9045 (Print) 1520-5762. DOI: 10.1080/03639045.2017.1310224.
34. Subramanian P, Rajnikanth PS, Kumar M, Chidambram K. In-Vitro and In-Vivo Evaluation of Supersaturable Self-Nanoemulsifying Drug Delivery System (SNEDDS) of Dutasteride. Current Drug Delivery, 2020, 17, 74-86; DOI: 10.2174/1567201816666191112111610.
35. Irahal IN, Darif D, Guenaou I, Hmimid F, Lahlou FA. Therapeutic Potential of Clove Essential Oil in Diabetes: Modulation of Pro-Inflammatory Mediators,Oxidative Stress and Metabolic Enzyme Activities. Chemistry and Biodiversity / volume 20, 2023; http:// doi.org/10.1002/cbdv.202201169.
36. Ganorkar AV, Askarkar SS, Gupta KR, Umekar MJ. Validated Stability Indicating and Assay Method Development of Linagliptin in Formulation by RP-HPLC Using Quality by Design. Orbital: Electron. J. Chem. 12 (2): 48-61, 2020; DOI: http://dx.doi.org/10.17807/orbital.v12i2.1194
37. Badran MM, Taha EI, Tayel MM, AL-suwayeh SA. Ultra-fine self nanoemulsifying drug delivery system for transdermal delivery of meloxicam: Dependency on the type of surfactants. Journal of Molecular Liquids 190 (2014) 16–22; http://dx.doi.org/10.1016/j.molliq.2013.10.015.

38. Buya AB, Beloqui A, Memvanga PB, Preat V . Self-Nano-Emulsifying Drug-Delivery Systems: From the Development to the Current Applications and Challenges in Oral Drug Delivery.Pharmaceutics (2020), 12, 1194; DOI: 10.3390/pharmaceutics12121194.
39. Suchaoin W, de Sousa IP, Netsomboon K, Lam HT, Laffleur F. Development and in vitro evaluation of zeta potential changing self-emulsifying drug delivery systems for enhanced mucus permeation. International Journal of Pharmaceutics (2016), 255-262; https://doi.org/10.1016/j.ijpharm.2016.06.045.
40. Cui W, Zhao H, Wang C, Chen Y, Luo C, Zhang S, Sun B, He Z. Co-encapsulation of docetaxel and cyclosporine A into SNEDDS to promote oral cancer chemotherapy. Drug Deliv., 2019. 26:1, 542-550; DOI: 10.1080/10717544.2019.1616237.
41. Khan AA, Atiya A, Akhtar S, Yadav Y, Qureshi KA, Jaremko M . Optimization of a Cefuroxime Axetil-Loaded Liquid Self-Nanoemulsifying Drug Delivery System: Enhanced Solubility, Dissolution and Caco-2 Cell Uptake. Pharmaceutics, 2022; http: // doi.org/10.3390/pharmaceutics14040772.
42. Park H, Ha ES, Kim MS. Current Status of Supersaturable Self-Emulsifying Drug Delivery Systems. Pharmaceutics, 2020, 12, 365; DOI: 10.3390/ pharmaceutics12040365**.**
43. Xua S, Daib W. Drug precipitation inhibitors in supersaturable formulations. International Journal of Pharmaceutics, 2013, 36-43; http://dx.doi.org/10.1016/j.ijpharm.2013.05.013.
44. Brouwers J, Vermeire K, Grammen C, Schols D, Augustijns P. Early identification of availability issues for poorly water-soluble microbicide candidates in biorelevant media: A case study with saquinavir. Antiviral Research 91 (2011) 217–223; http://doi.org/10.1016/j.antiviral.2011.06.001.
45. Qiu C, Gao LN, Yan K, Cui YL, Zhang Y. A promising antitumor activity of evodiamine incorporated in hydroxypropyl- β- cyclodextrin: pro- apoptotic activity in human hepatoma HepG2 cells. Chemistry Central Journal (2016) 10:46; DOI 10.1186/s13065-016-0191-y.
46. Quan G, Niu B, SinghV, Zhou Y, Wu CY, Pan X, Wu C. Supersaturable solid self-microemulsifying drug delivery system: precipitation inhibition and bioavailability enhancement. International Journal of Nanomedicine (2017):12 8801–8811; DOI: 10.2147/IJN.S149717.
47. Jain A, Kaur R, Beg S, Kushwah V, Jain S, Singh B. Novel cationic supersaturable nanomicellar systems of raloxifene hydrochloride with enhanced biopharmaceutical attributes. Drug Delivery and Translational Research, (2018); https://doi.org/10.1007/s13346-018-0514-8.
48. Chen XL, Liang XL, Zhao GW, Zeng QY, Dong W. Improvement of the bioavailability of curcumin by a supersaturatable self nanoemulsifying drug delivery system with incorporation of a hydrophilic polymer: in vitro and in vivo characterization.Journal of Pharmacy and Pharmacology, 2021, Vol 73, 641–652; DOI:10.1093/jpp/rgaa073.
49. Barden AT, Engela RE, Campanharo SC, Volpato MN, Schapoval EV. Characterization of linagliptin using analytical techniques, Drug Anal Res, 2017; 01, n.2, 30-37; DOI: http:// doi.org/10.22456/2527-2616.79220.